A)

Variable	Correlation with RB % cells positive Rho (p); n	Correlation with RB weighted intensity score Rho (p); n
Ki67	0.14 (0.31); 58	0.13 (0.35); 58
PTEN	0.16 (0.26); 54	0.18 (0.19); 54
AR	-0.07 (0.59); 66	-0.09 (0.48); 66

B)

		RB (% cells positive)		RB Weighted Intensity Score	
Treatment	Orchiectomy (n=55)	75 (46,85)	p=0.86	1.19 (0.6,1.5)	p=0.82
	LHRH (n=32)	70 (40, 84.5)		1.04 (0.4,1.49)	

		Ki67 (% cells positive)	
Treatment	Orchiectomy (n=55)	9 (3,19)	p=0.41
	LHRH (n=32)	9 (6, 20)	

Supplemental Table 1. A) Spearman correlation comparing RB status with other clinical correlates. Correlation with both percent RB positive and weighted RB intensity score shown. B) Association between treatment and RB positivity (*top*) or Ki-67 positivity *(bottom)* assessed through Wilcoxon rank sum testing.

A)

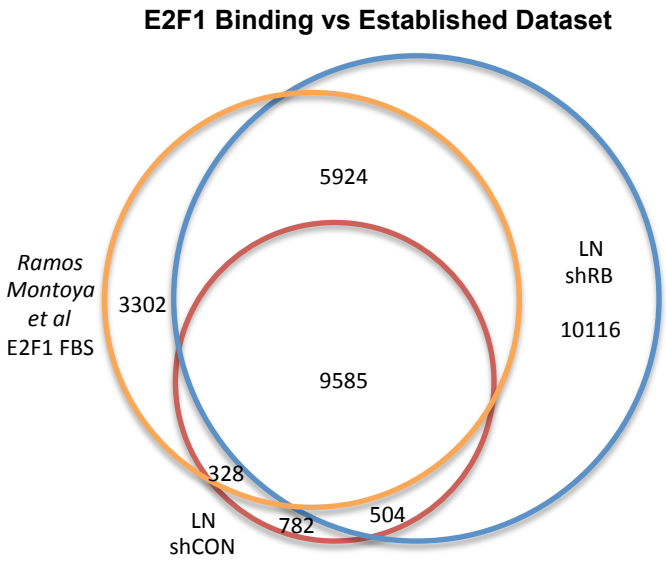

B)

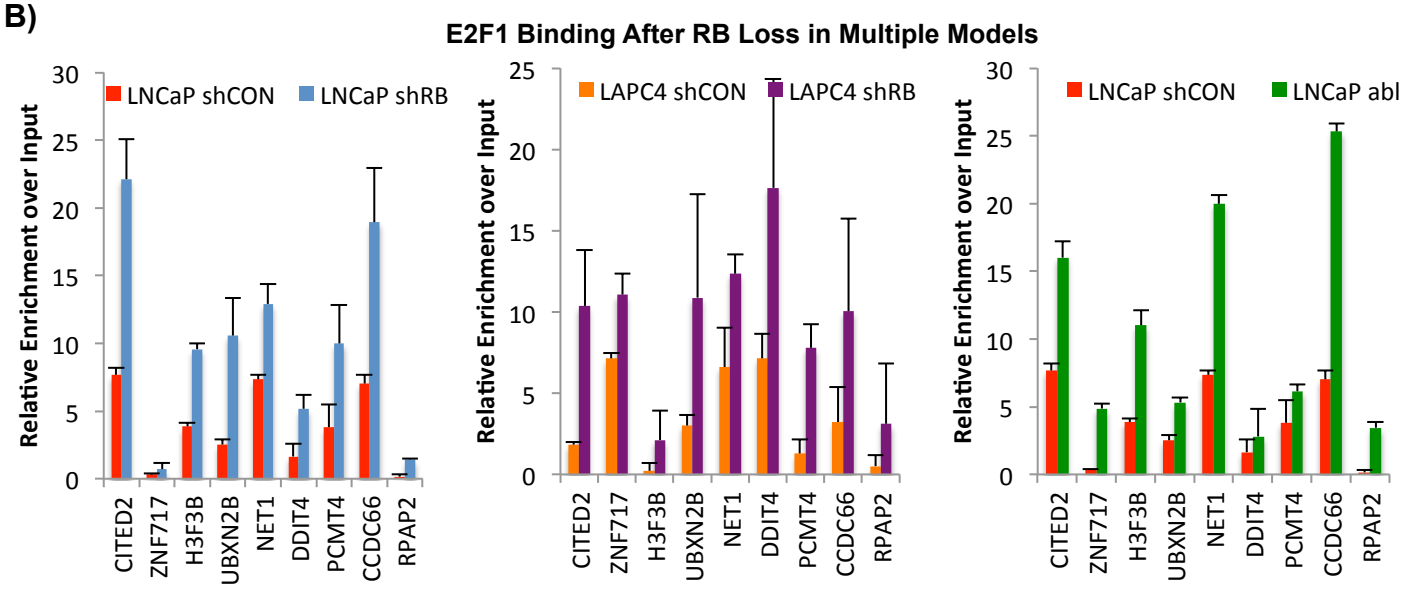

C) E2F1 Binding – LN abl vs LN shRB

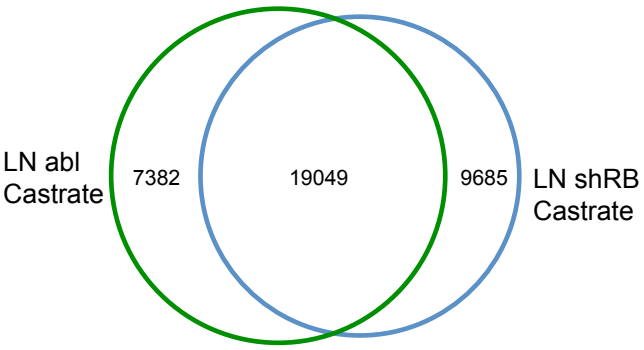

Supplemental Figure 2. A) E2F1 binding in shCON or shRB in castrate conditions compared to previously identified E2F1 cistrome published by Ramos-Montoya et al. B) Validation of E2F1 binding in LNCaP shCON/shRB pairs, LAPC4 shCON/shRB pairs, and LNCaP vs LNCaP-abl (which lose RB during progression to castrate resistance). C) Overlap in E2F1 binding in shRB LNCaP and LNCaP abl (Xu et al 2016).

LN shCON Castrate
Exclusive Binding

Motif Name	P-value
E2F4	1.00E-106
E2F6	1.00E-103
Fox:Ebox	1.00E-90
E2F1	1.00E-83
Foxa2	1.00E-82
CTCF	1.00E-73
FOXA1	1.00E-66
FOXA1	1.00E-65
E2F7	1.00E-64
BORIS	1.00E-47
E2F	1.00E-43
FOXP1	1.00E-35

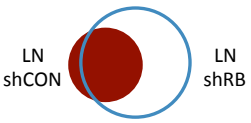

LN shCON Castrate
All Binding

Motif Name	P-value
E2F4	1e-427
NFY	1e-330
Elk4	1.00E-297
Elk1	1.00E-283
Sp1	1.00E-278
ELF1	1.00E-269
ETS	1.00E-265
E2F6	1.00E-254
E2F1	1.00E-249
Fli1	1.00E-248
GFY-Staf	1.00E-230
GABPA	1.00E-215
E2F7	1.00E-213
CTCF	1.00E-201
GFY	1.00E-185
NRF1	1.00E-172
ETV1	1.00E-170
NRF	1.00E-164
ETS1	1.00E-153
ERG	1.00E-133
EWS:FLI1-fusion	1.00E-116
YY1	1.00E-113
KLF5	1.00E-109
E2F	1.00E-105
EHF	1.00E-102
CRE	1.00E-93
BORIS	1.00E-89
ELF5	1.00E-84
SPDEF	1.00E-68
ZNF143|STAF	1.00E-62
RFX	1.00E-56
MYB	1.00E-53
JunD	1.00E-53
E-box	1.00E-53
Stat3	1.00E-53
BMYB	1.00E-53
Rfx2	1.00E-51
Foxa2	1.00E-42
Klf4	1.00E-39
Rfx1	1.00E-38
AMYB	1.00E-37
GFX	1.00E-36
Stat3+il21	1.00E-36
Rfx5	1.00E-34
Atf2	1.00E-33
STAT4	1.00E-32
USF1	1.00E-29
Fox:Ebox	1.00E-29
CLOCK	1.00E-28
X-box	1.00E-27
Maz	1.00E-26
Atf1	1.00E-26
c-Myc	1.00E-26
bHLHE40	1.00E-25
STAT1	1.00E-25
FOXA1	1.00E-25
FOXP1	1.00E-25
FOXA1	1.00E-25
Foxo1	1.00E-24
MITF	1.00E-23
PU.1-IRF	1.00E-22
Nanog	1.00E-22
ZBTB33	1.00E-22
STAT5	1.00E-20
EWS:ERG-fusion	1.00E-20
c-Jun-CRE	1.00E-20
TATA-Box	1.00E-20

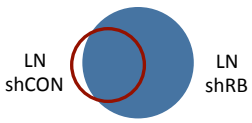

LN shRB Castrate
All Binding

Motif Name	P-value
CTCF	1e-2184
BORIS	1e-1161
Elk4	1.00E-188
Fli1	1.00E-174
Elk1	1.00E-172
ELF1	1.00E-152
NFY	1.00E-147
Sp1	1.00E-147
GABPA	1.00E-144
ETS	1.00E-139
E2F4	1.00E-129
ETV1	1.00E-123
ERG	1.00E-106
Foxa2	1.00E-95
GFY-Staf	1.00E-94
Fox:Ebox	1.00E-93
NRF	1.00E-88
ETS1	1.00E-87
GFY	1.00E-86
E2F6	1.00E-81
NRF1	1.00E-80
FOXA1	1.00E-78
NF1	1.00E-76
EWS:FLI1-fusion	1.00E-76
SPDEF	1.00E-76
EHF	1.00E-74
KLF5	1.00E-73
FOXA1	1.00E-72
NF1-halfsite	1.00E-72
YY1	1.00E-65
RFX	1.00E-64
FOXP1	1.00E-64
Rfx2	1.00E-62
E2F7	1.00E-58
ELF5	1.00E-58
BMYB	1.00E-57
Stat3	1.00E-56
AMYB	1.00E-55
Rfx1	1.00E-53
CRE	1.00E-52
E2F1	1.00E-51
CTCF-SatelliteElement	1.00E-45
Stat3+il21	1.00E-45
MYB	1.00E-44
Foxo1	1.00E-43
Tlx?	1.00E-43
STAT4	1.00E-42
E2F	1.00E-39
Rfx5	1.00E-32
E-box	1.00E-32
X-box	1.00E-32
Tcf12	1.00E-31
NF1:FOXA1	1.00E-30
Arnt:Ahr	1.00E-30
NeuroD1	1.00E-30
Unknown-ESC-element	1.00E-29
Rbpj1	1.00E-29
Klf4	1.00E-28
SCL	1.00E-26
GRHL2	1.00E-26
REST-NRSF	1.00E-26
Maz	1.00E-25
Smad3	1.00E-23
Bcl6	1.00E-23
Lhx3	1.00E-23
MafA	1.00E-23
GFX	1.00E-22
STAT1	1.00E-22
STAT5	1.00E-20
Unknown	1.00E-20

LN shRB Castrate
Exclusive Binding

Motif Name	P-value
CTCF	1e-2422
BORIS	1e-1489
Foxa2	1.00E-100
Fox:Ebox	1.00E-96
NF1	1.00E-86
FOXA1	1.00E-82
FOXA1	1.00E-81
NF1-halfsite	1.00E-79
FOXP1	1.00E-61
SCL	1.00E-55
Unknown-ESC-element	1.00E-48
Tlx?	1.00E-42
Tcf12	1.00E-42
Ascl1	1.00E-40
NeuroD1	1.00E-38
SPDEF	1.00E-37
REST-NRSF	1.00E-36
Foxo1	1.00E-29
Fli1	1.00E-29
ERG	1.00E-28
CTCF-SatelliteElement	1.00E-28
GRHL2	1.00E-27
Stat3	1.00E-26
Bcl6	1.00E-24
ETV1	1.00E-23
GABPA	1.00E-22
BMYB	1.00E-22
NF1:FOXA1	1.00E-21
Stat3+il21	1.00E-20
AR-halfsite	1.00E-20

Supplemental Figure 3: RB loss results in differential E2F1 binding associated motif enrichment in castrate conditions. Briefly, Homer was used to find enriched motifs using a 1kb window around the center of binding, using the binding datasets indicated by the shaded region of each venn diagram.

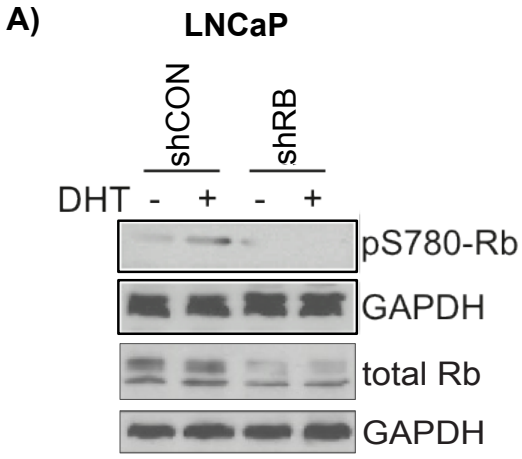

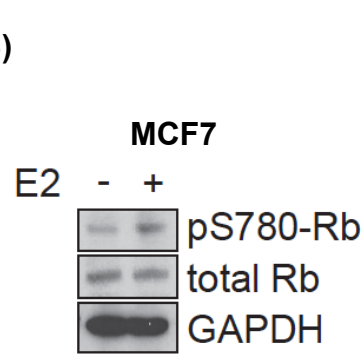

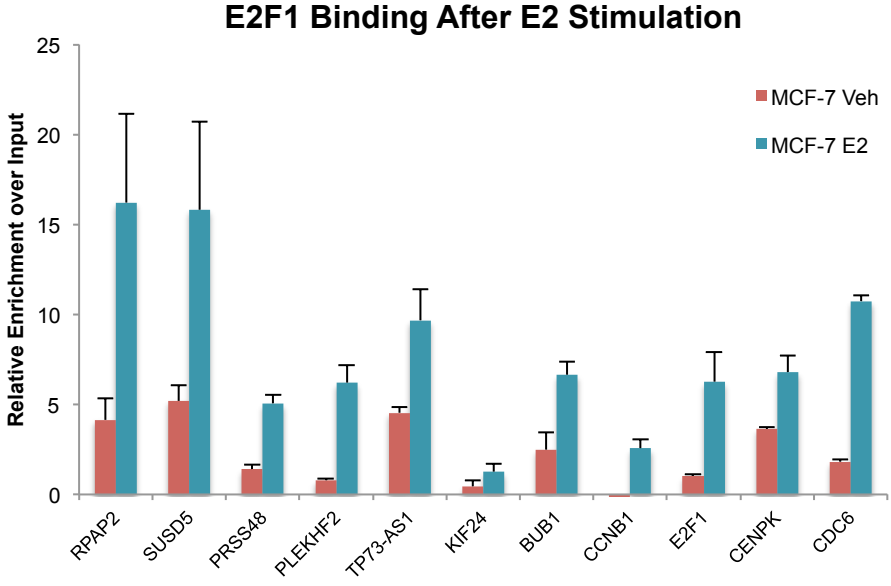

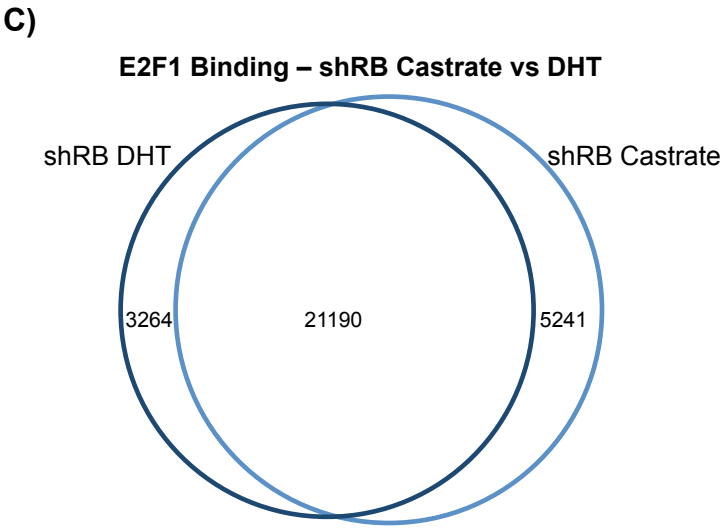

Supplemental Figure 4. A) Immunoblot of androgen induced RB phosphorylation after 3 hours of DHT stimulation B) Estrogen treatment in MCF7 cell models elicit similar phosphorylation of RB compared to DHT treatment (*left*) and MCF7 cells exhibit similar expansion of E2F1 binding after E2 treatment at sites of gained E2F1 binding after DHT stimulation in LNCaP cells (*right*). C) E2F1 binding overlap in LNCaP shRB cells in castrate and DHT stimulated conditions.

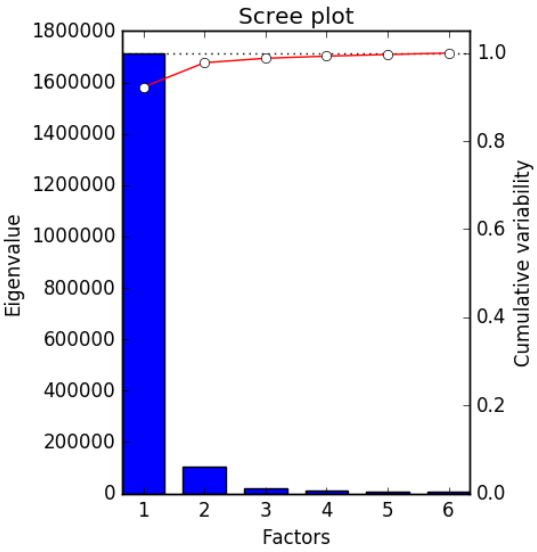

Supplemental Figure 5. Scree plot indicating variability explained by the indicated factors. Red line indicates cumulative variability explained by each individual component.

A)

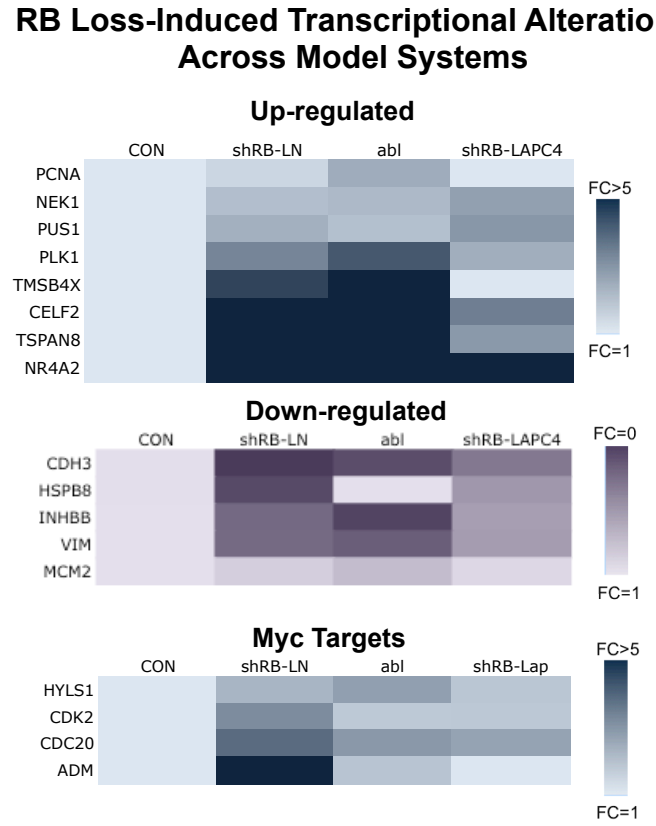

B)

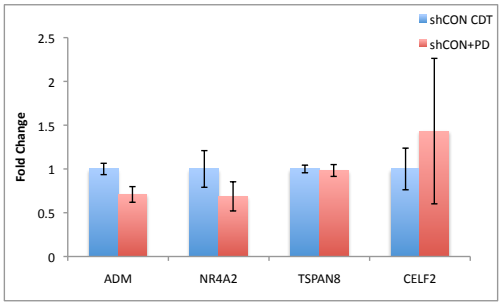

C)

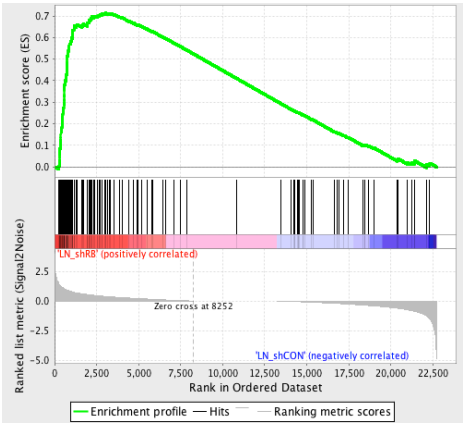

D)

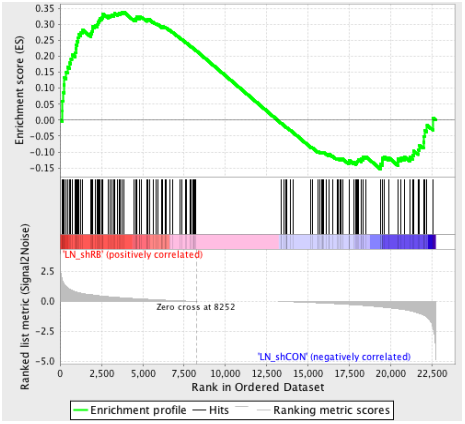

Supplemental Figure 6. A) Validation of differentially expressed targets after RB loss in multiple models of RB loss both upregulated (*top),* downregulated (*middle)*, and Myc targets from GSEA enrichment (*bottom*). B, C) Gene set enrichment analysis utilizing previously published signature of RB loss (Ertel *et al* 2010) or CRPC AR targets (Sharma *et al* 2013). D) Transcriptional alterations for genes validated in A after CDK4/6 inhibitor treatment in castrate conditions.

A)

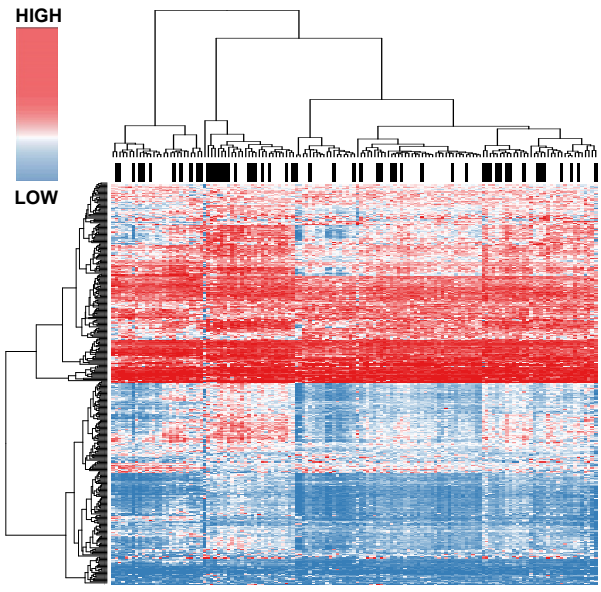

B)

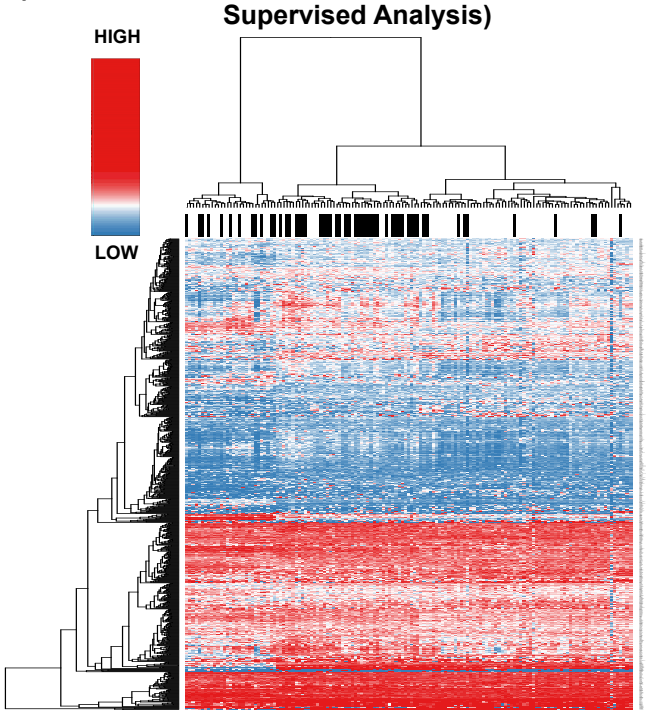

C)

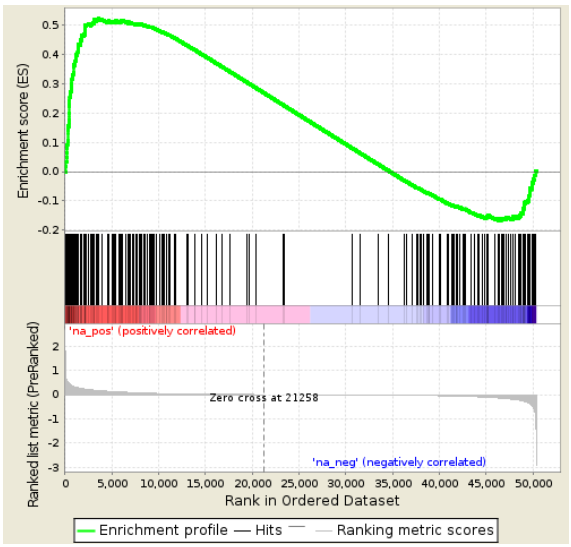

Supplemental Figure 7. RB loss results in differential E2F1 binding associated motif enrichment in castrate conditions. A) Hierarchical clustering of normalized expression data of all genes with a nearby E2F1 binding site from 144 SU2C CRPC samples (1-Pearson's correlation coefficient for columns and Euclidean distance for rows were used as distance measures). The annotation track reports the genomic status of RB1 (black: SCNA alteration; white: no SCNA alteration). B) Hierarchical clustering of normalized expression data of differentially expressed genes (RB altered vs RB WT) identified through utilizing only SU2C expression data. C) GSEA enrichment of genes up-regulated by RB loss and exclusively bound by E2F1 in the current model within genes from analysis in B.

Supplemental Methods:

Primers utilized in study:

ChIP Primers	Forward	Reverse
CITED2	TTGTCCCGTTCATCTGGTGG	GCTGCAGAAGCTCAACAACC
ZNF717	GGAGGAAAATGGCGGAGTGG	TGGGCAAAACAGAATGTCCG
H3F3B	ACGACGAATCTCTCGAAGCG	TTCGGGGCGTCTTTCTTAGG
UBXN2B	GATTTGCAGGTGAGGCGAGG	ACCACCACAGTGTCAAGACC
NET1	CTGTCCTACTTGAACCCAGC	ATCAATCCACACCGAGTCAGC
DDIT4	AGTCCTTATAGGCTGCTCCG	TAGGACCCACACACAGAAGG
PCMT1	CTCAGAAAGGGACACGCAGC	CAAGAGTGAGACCACCTCCC
CCDC66	AACAAACGGCATACGCAACC	TGACGACCACCTTGCTTACC
RPAP2	CCACAACTCCACTTACCGGC	GATCCTTGCTCCTACCTGCG
BUB1	TTGAAACTTGGCGGCTAGGG	TCCCGTACCTACCTCAGAGC
KIF24	CCTAACAGTCCCGTCAACCC	AACCGATTCCTTGGATGCCC
CENPK	CCGGCGATAAGGGTTTCACC	CAGTCTTCTGTCAGCGTCCG
RPAP2	CCACAACTCCACTTACCGGC	GATCCTTGCTCCTACCTGCG
SUSD5	GCTTTGGAGGAATACTGCACG	AGCATGTAAATGGCTCCTGC
PRSS48	TAAACGGGATAGGAAGAGGGG	ACACTGGAATATCGTGAAAAGGC
PLEKHF2	ACTTTCTAAGGGCTGGTCGG	TTGTCCATGTGTGAGGTCGG
BIRC2	TACGGATAGTCCCCGTTCCC	ACTCTGACGCACGATGACG
C1GALT1	CAGACCCCTTCGCATTAGGG	CCAGATTATTCCCCGGCAGC
HMGA1	CCTATAGCAGGCTCACAAGGG	TGTGTCAAAGCAGCGTTTCG
TP73-AS1	CTCCCATCTAGGGATCCACACC	GTTGTTGCGGGATCTCACAGG
PRDM4	TGCTTTGTTCCTCATCCGGG	TGGCTGAGGATCCGGAAACG
E2F1	AGGAACCGCCGCCGTTGTTCCCGT	CTGCCTGCAAAGTCCCGGCCACTT
CCNB1	CGATCGCCCTGGAAACGCATTC	CCAGCAGAAACCAACAGCCGTTC
CDC6	GTGCAGGATCCTTCTCACGTCTCTCAC	AAAGGCTCTGTGACTACAGCCAAT
mRNA Primers	**Forward**	**Reverse**
PCNA	TAGCCACATTGGAGATGCTG	CAGTGGAGTGGCTTTTGTGA
NEK1	AGGTGGCTCTCCATCAAAGC	TCACAAGTTGACCTCCTGCC
PUS1	GATTCTGGGACTGAAGCGGG	ATTGTGGAAGTTGTGCGTGC
PLK1	CAAGCTGGGCAACCTTTTCC	GATCCTCAGCCTCCTCTTGC
TMSB4X	CTCGCTTCGCTTTTCCTCCG	GTACAGTGCATATTGGCGGC
CELF2	AGAAGGAAGGTCCAGAGGGG	GCTTGGATAGCAGCTTGTGC
TSPAN8	CAAGAAGAGTTTAAATGCTGCG	AGGCACATAATTCAGGATAGTG
NR4A2	ACTATTCCAGGTTCCAGGCG	GGGTACGAAGTTCTGGGAGC
CDH3	GTCTCAGTTCCCCCTTCAGC	GACTCATAGCCTGTCTCCGC
HSPB8	CACAAAGAAAATCCAGCTTCCTGC	AGAGAAGCCCTAGGGTTGGG
INHBB	AGCTTCGCCGAGACAGATGG	CGTAGGGCAGGAGTTTCAGG
VIM	TCCACGAAGAGGAAATCCA	CAGGCTTGGAAACATCCAC
MCM2	CAACACTGCCAATGGCTTCC	CTTGCCACCTGGGTTTTTGG
HYLS1	GTGGAAATGAAAGCAGAAGGTCC	TTTCGGAGTCTTTGGGAGGC
CDK2	CTCATCAAGAGCTATCTGTTCC	TTTAAGGTCTCGGTGGAGG
CDC20	ATTTGGAACGTCTGCTCAGG	CTTGGCCATGGTTGGATACT
ADM	CCCTGATGTACCTGGGTTCG	CATCCGGACTGCTGTCTTCG
GAPDH	CCAGGTGGTCTCCTCTGACTTC	TCATACCAGGAAATGAGCTTGACA

ChIP-Seq Analyses: Alignment performed using Bowtie and peak calling was completed using MACS2 using a Q value cutoff of 0.01 (1). Venn Diagrams for binding overlaps generated using pybedtools v0.7.8 and bedtools v2.24.0 (2, 3). Heatmaps for binding intensity generated using DeepTools v2.2.4 (4). Cis-regulatory element analysis performed using CEAS v1.0.2 (5). Motif analyses were generated through Homer v4.8.3 (6). *Denovo* analysis was performed using a 50bp window around indicated binding, while known analysis was performed using a 1000bp window around indicated binding.

RNA-Seq Analyses: RNA-Seq alignment was performed using STAR v2.5.2a (7). Differential gene expression was generated using edgeR v3.16.5 (8). Gene set enrichment analysis completed through GSEA using gene sets from the Molecular Signature Database (9). Binding to gene analysis achieved through BETA v1.0.7 using a 30kb window around center of binding (10). Circos plot created using Circos v0.69-3 (11).

ATAC-Seq Analyses: ATAC-Seq analysis was performed utilizing the ENCODE ATAC-Seq processing pipeline (https://www.encodeproject.org/atac-seq/). Downstream analyses including PCA and signal plots were obtained using DeepTools (4).

SU2C/PCF CRPC Tumor Cohort - RNA-seq data analysis: Processed SU2C/PCF (12) RNA-seq data (n = 149) were downloaded from cBioPortal (13). Samples with neuroendocrine molecular features as assessed by elevated Integrated NEPC Score (14) (greater than or equal to 0.25) were excluded for downstream analysis (n=5). To nominate genes with concordant expression with respect to RB1 status in the SU2C/PCF CRPC cohort (RB1 altered, n = 53, vs RB1 wt, n = 64) and the study model, in addition to the same deregulation versus, at least one of the following criteria was requested to be satisfied, i) significant differential expression (p-value < 0.1, Wilcoxon Mann Whitney test) ii) significant association between expression level and genomic status of RB1 (wt, hemi and homozygous; p-value <

0.1, Anova test), while genes meeting this criteria were also required to exhibit the same sign FC to ensure concordance between datasets.

SU2C/PCF CRPC Tumor Cohort - Identification of genomic status: Allele-specific copy number genomic status of the indicated genes were assessed from the Whole Exome Sequencing (WES) SU2C/PCF cohort as previously described (15).

Copy Number alteration and ctDNA procedure: Circulating cell free DNA from a cohort of CRPC patients was harvested, isolated, and sequenced as previously described (16). Analysis of alteration co-occurrence was generated using GenVisR bioconductor package(17).

Immunohistochemistry – Tampere Cohort: IHC analyses for Ki-67 and RB1 were performed on CRPC TMAs as previously described (18, 19).

Immunohistochemistry - The Institute of Cancer Research CRPC Cohort: Tissue samples were obtained from CRPC patients through CCR2472 -Marsden ethics committee approved protocol for sample collection. FFPE samples were cut at 4um thick sections onto superfrost glass slides for immunohistochemical staining. Primary anti-RB1 (mouse monoclonal, Clone G3-245, BD Biosciences, San Jose – CA, USA) and anti-Ki67 (mouse monoclonal, Clone MIB-1, Agilent-Dako, Santa Clara – CA, USA) antibodies were diluted 1:100. Germinal centers in associated lymphoid tissue of the appendix was used as a positive control and striated muscle and cell line MDA-MB-468 were used as negative controls for ki67 and RB1 respectively. Heat based antigen retrieval was performed by boiling slides in a pressure cooker at 125ºC for 2 minutes then 90°C for 1 minute in a pH 6 citrate buffer solution. Endogenous peroxide was blocked using a 3% H2O2 solution. Non-specific staining was blocked using Dako protein block serum-free X0909. The Dako-Envision kit (Agilent-Dako, Santa Clara – CA, USA) was used for reaction visualization. Ki-67 staining was semi-quantitatively scored by one pathologist

(DNR) blinded to RB1 status as a percentage determined by (proportion of positive tumor cells)/(total number of tumor cells)x100. RB1 staining was semiquantitatively assessed by assigning a proportion of tumour cells in each section into four tiers representing: no staining (0), weakly positive (+1), moderately positive (+2), and strongly positive (+3).

TMA IHC Analysis - Tampere and The Institute of Cancer Research Cohort: TMA RB vs Ki67 Correlation was associated as follows. RB status was summarized in two ways. First, the total percentage of cells staining 1 or greater, and, second, as a weighted average of the intensity scores where the weights were the percentage of cells staining at that intensity. Spearman correlation coefficients were calculated to assess the association between RB status and Ki67, PTEN, and AR where applicable. Grouped scatter-plot samples were grouped by IHC score, and percent of each tumor null for RB plotted in respective IHC score bin.

Cell Culture and Treatment: Isogenic cell lines for RB loss were generated from LNCaP cells originally purchased from ATCC as previously described (20), with cells maintained as described previously (21). Briefly, in castrate conditions, phenol red-free media supplemented with 5% charcoal dextran-treated serum (CDT) was used. All experiments utilizing Dihydrotestosterone (DHT) used DHT obtained from Sigma-Aldrich (St. Louis, MO, USA), which was dissolved in ethanol prior to use. Breast cancer MCF-7 cells were originally purchased from ATCC and were maintained and propagated in Dulbecco's Modified Eagle Medium (DMEM) supplemented with 10% FBS and 1% P/S. Prior to harvest, MCF-7 cells were hormone deprived for 3 days, and subsequently treated with 10 nM (final concentration) estradiol for three hours before harvest.

References

1. Zhang Y, Liu T, Meyer CA, Eeckhoute J, Johnson DS, Bernstein BE, Nusbaum C, Myers RM, Brown M, Li W, et al. Model-based analysis of ChIP-Seq (MACS). *Genome Biol.* 2008;9(9):R137.

2. Dale RK, Pedersen BS, and Quinlan AR. Pybedtools: a flexible Python library for manipulating genomic datasets and annotations. *Bioinformatics.* 2011;27(24):3423-4.
3. Quinlan AR, and Hall IM. BEDTools: a flexible suite of utilities for comparing genomic features. *Bioinformatics.* 2010;26(6):841-2.
4. Ramirez F, Dundar F, Diehl S, Gruning BA, and Manke T. deepTools: a flexible platform for exploring deep-sequencing data. *Nucleic Acids Res.* 2014;42(Web Server issue):W187-91.
5. Ji X, Li W, Song J, Wei L, and Liu XS. CEAS: cis-regulatory element annotation system. *Nucleic Acids Res.* 2006;34(Web Server issue):W551-4.
6. Heinz S, Benner C, Spann N, Bertolino E, Lin YC, Laslo P, Cheng JX, Murre C, Singh H, and Glass CK. Simple combinations of lineage-determining transcription factors prime cis-regulatory elements required for macrophage and B cell identities. *Mol Cell.* 2010;38(4):576-89.
7. Dobin A, Davis CA, Schlesinger F, Drenkow J, Zaleski C, Jha S, Batut P, Chaisson M, and Gingeras TR. STAR: ultrafast universal RNA-seq aligner. *Bioinformatics.* 2013;29(1):15-21.
8. Robinson MD, McCarthy DJ, and Smyth GK. edgeR: a Bioconductor package for differential expression analysis of digital gene expression data. *Bioinformatics.* 2010;26(1):139-40.
9. Subramanian A, Tamayo P, Mootha VK, Mukherjee S, Ebert BL, Gillette MA, Paulovich A, Pomeroy SL, Golub TR, Lander ES, et al. Gene set enrichment analysis: a knowledge-based approach for interpreting genome-wide expression profiles. *Proc Natl Acad Sci U S A.* 2005;102(43):15545-50.
10. Wang S, Sun H, Ma J, Zang C, Wang C, Wang J, Tang Q, Meyer CA, Zhang Y, and Liu XS. Target analysis by integration of transcriptome and ChIP-seq data with BETA. *Nat Protoc.* 2013;8(12):2502-15.
11. Krzywinski M, Schein J, Birol I, Connors J, Gascoyne R, Horsman D, Jones SJ, and Marra MA. Circos: an information aesthetic for comparative genomics. *Genome Res.* 2009;19(9):1639-45.
12. Robinson D, Van Allen EM, Wu YM, Schultz N, Lonigro RJ, Mosquera JM, Montgomery B, Taplin ME, Pritchard CC, Attard G, et al. Integrative clinical genomics of advanced prostate cancer. *Cell.* 2015;161(5):1215-28.
13. Cerami E, Gao J, Dogrusoz U, Gross BE, Sumer SO, Aksoy BA, Jacobsen A, Byrne CJ, Heuer ML, Larsson E, et al. The cBio cancer genomics portal: an open platform for exploring multidimensional cancer genomics data. *Cancer Discov.* 2012;2(5):401-4.
14. Beltran H, Prandi D, Mosquera JM, Benelli M, Puca L, Cyrta J, Marotz C, Giannopoulou E, Chakravarthi BV, Varambally S, et al. Divergent clonal evolution of castration-resistant neuroendocrine prostate cancer. *Nat Med.* 2016;22(3):298-305.
15. Mu P, Zhang Z, Benelli M, Karthaus WR, Hoover E, Chen CC, Wongvipat J, Ku SY, Gao D, Cao Z, et al. SOX2 promotes lineage plasticity and antiandrogen resistance in TP53- and RB1-deficient prostate cancer. *Science.* 2017;355(6320):84-8.
16. De Laere B, van Dam PJ, Whitington T, Mayrhofer M, Diaz EH, Van den Eynden G, Vandebroek J, Del-Favero J, Van Laere S, Dirix L, et al. Comprehensive Profiling of the Androgen Receptor in Liquid Biopsies from Castration-resistant Prostate Cancer Reveals Novel Intra-AR Structural Variation and Splice Variant Expression Patterns. *Eur Urol.* 2017.
17. Skidmore ZL, Wagner AH, Lesurf R, Campbell KM, Kunisaki J, Griffith OL, and Griffith M. GenVisR: Genomic Visualizations in R. *Bioinformatics.* 2016;32(19):3012-4.

18. Augello MA, Burd CJ, Birbe R, McNair C, Ertel A, Magee MS, Frigo DE, Wilder-Romans K, Shilkrut M, Han S, et al. Convergence of oncogenic and hormone receptor pathways promotes metastatic phenotypes. *J Clin Invest.* 2013;123(1):493-508.
19. Sharma A, Yeow WS, Ertel A, Coleman I, Clegg N, Thangavel C, Morrissey C, Zhang X, Comstock CE, Witkiewicz AK, et al. The retinoblastoma tumor suppressor controls androgen signaling and human prostate cancer progression. *J Clin Invest.* 2010;120(12):4478-92.
20. Sharma A, Comstock CE, Knudsen ES, Cao KH, Hess-Wilson JK, Morey LM, Barrera J, and Knudsen KE. Retinoblastoma tumor suppressor status is a critical determinant of therapeutic response in prostate cancer cells. *Cancer Res.* 2007;67(13):6192-203.
21. McNair C, Urbanucci A, Comstock CE, Augello MA, Goodwin JF, Launchbury R, Zhao SG, Schiewer MJ, Ertel A, Karnes J, et al. Cell cycle-coupled expansion of AR activity promotes cancer progression. *Oncogene.* 2016.